The behavior on the two borders, left and right, of the transition superconductors, namely, in the column headed 3 and again in columns 8 and 9, is the opposite to the behavior of the elements in the center. In the center the elements in the middle row having $4d$ electrons, such as Zr, Nb, Mo, and Tc, have the highest transition temperatures in their respective column, while at the fringes the $5d$ electron superconductors of the last row have the highest transitions, such as La, Os, and Ir. For the last three, clearly any dependence on mass goes—if anywhere—in the opposite direction to what might be expected from a regular isotope effect. Thus, not only Ru and Os, but also La and Ir, might be expected to have at least a vanishing isotope effect. This should also be true for Sc, Y, and Rh once their superconductivity has been detected, as may happen in the future.

The columns 3, 8, and 9 are also distinguished by another feature. While in the center of the periodic system the electronic specific heat, γ, and the superconducting transition temperature seem to be somewhat related in the way that a high T_c goes with a high γ, this behavior is precisely the *opposite* for the three groups of elements just mentioned. For almost all of these elements at both boundaries, superconductivity seems to *vanish* upon an increase of the electronic specific heat. Since there is no theory at present for the second mechanism the significance of this observation is not clear.

We would like to thank A. M. Clogston, P. A. Wolff, and P. W. Anderson for informative discussions concerning the isotope effect, and Mrs. V. B. Compton for her helpful x-ray investigations, and L. D. Longinotti for his careful help in preparing the samples.

Theory of Cyclotron Resonance in Strained Silicon Crystals*

Hiroshi Hasegawa†

Department of Physics, University of California, San Diego, La Jolla, California

(Received 13 September 1962)

The valence band structure in silicon single crystals subjected to an external uniaxial stress is investigated. The cyclotron resonance line for holes in such crystals is predicted to display a significant shift with increasing stress, if the split band populated with holes is associated with the quantum number $M_J = \pm\frac{1}{2}$. This strain-induced shift is characterized by the following properties: (a) Its magnitude is of the order of 10% of the frequency for strains of the order of 2×10^{-3}; (b) it is anisotropic with respect to the relative orientation of the external magnetic field to that of the stress; (c) it must be absent if the band populated with holes is associated with the quantum number $M_J = \pm3/2$. These properties in conjunction with the experimentally determined shifts, presented in the paper by Hensel and Feher, lead to a unique assignment of the band parameters which had been left ambiguous by previous experiments. A discussion of the line shape of hole resonance in a deformed crystal is also presented.

1. INTRODUCTION

SINCE the first cyclotron resonance experiments were successfully carried out in germanium and silicon crystals by Dresselhaus, Kip, and Kittel,[1] and by Lax, Zeiger, and Dexter,[2] considerable information has accumulated from experiments about the energy band structures of these crystals. This information has stimulated extensive band-theoretical studies.[3] One of the major endeavors in the experimental investigations has been to elucidate the two degenerate valence bands

and also the third band that is split off from the first two by spin-orbit interactions.

Recently, Hensel and Feher have performed microwave cyclotron resonance experiments on silicon crystals strained by uniaxial stresses and, thus, have been able to determine the valence band inverse mass parameters as well as the band-splitting deformation potentials to an accuracy greater than previously. Full accounts of the experimental results are given in their paper.[4] Their preliminary results have already been reported elsewhere.[5] In the present paper we investigate theoretically the structure of the valence band in silicon influenced by external stresses in order to obtain cyclotron resonance frequencies of holes under such conditions.

The present investigation was undertaken in an attempt to settle a question raised in reference 5 con-

* Supported in part by the Office of Naval Research.

† Present address: Department of Physics, University of Tokyo, Tokyo, Japan.

[1] G. Dresselhaus, A. F. Kip, and C. Kittel, Phys. Rev. 98, 368 (1955).

[2] B. Lax, H. J. Zeiger, and R. N. Dexter, Physica 20, 818 (1954); Phys. Rev. 104, 637 (1956). For recent results see B. Lax and J. G. Mavroides, in *Solid State Physics*, edited by F. Seitz and D. Turnbull (Academic Press Inc., New York, 1960), Vol. 11, p. 261.

[3] W. Kohn, in *Proceedings of the International Conference on Semiconductor Physics, Prague, 1960* (Czechoslovakian Academy of Sciences, Prague 1961), p. 15.

[4] J. C. Hensel and G. Feher, following paper [Phys. Rev. 129, 1041 (1963)]. It is frequently referred to with the abbreviation H-F in the present paper.

[5] J. C. Hensel and G. Feher, Phys. Rev. Letters 5, 307 (1960).

cerning the lack of information about the signs of the deformation potentials, D_u and D_u'. These, it was found, have a close correlation with the signs of certain effective mass parameters in the silicon valence band. The uncertainty of these latter signs, in particular that of $B = \frac{1}{3}(L-M)$ defined in reference 1, has been recognized to allow two entirely different interpretations of the structure of the band and, thus, has been one of the crucial points in the band theory of silicon. In Sec. 2 a brief account will be given, therefore, of the above-mentioned problem of the sign ambiguity. We will then calculate all possible factors to be taken into account in determining the effective masses of holes in the deformed band. In Sec. 3 we calculate shifts of the effective masses due to strain-induced admixtures between the valence band edge and the spin-orbit split-off band at the center of the Brillouin zone. We shall show that the presence or absence of the shift distinguishes the nature of the two decoupled bands in terms of the quantum number M_J, and that its identification by experiment yields a possibility of fixing the signs of D_u and D_u'. This result can then be combined with the analysis of reference 5 to determine the signs of the band parameters uniquely. In Sec. 4 we examine the effects of k^4 terms on the resonance line, and in Sec. 5 some supplementary calculations are added.

The results of Sec. 4 show that an effect of the incompleteness of the decoupling of the bands gives rise to an additional shift, broadening, and asymmetry of the cyclotron resonance line. Thus, a study of the line shape is included that will improve the accuracy of the determination of the effective mass parameters.

Over-all considerations presented in Secs. 3–5 lead to our final conclusion: The strain-induced mass shift of Sec. 3 is distinctive and large enough so that its identification allows us to uniquely assign all the parameters.[6]

2. SIGN AMBIGUITY OF THE PARAMETER B FOR SILICON

It is well known from usual band theory that an effective mass tensor of an energy band at a particular point in the first Brillouin zone is determined by the $\mathbf{k} \cdot \mathbf{p}$ perturbation formula. For its evaluation it is necessary to know the positions of the energy levels at the same point and the matrix elements of electron momentum between these levels. For the valence states $\Gamma_{25'}$ which are relevant to the hole resonance in a diamond-type crystal it has been shown that the

three effective mass parameters L, M, and N are determined by the perturbations in which the four different representations Γ_{15}, $\Gamma_{2'}$, $\Gamma_{12'}$, and Γ_{25} furnish nonvanishing matrix elements.[1]

In the earlier experiments of cyclotron resonance on holes in germanium[1] the deduced constants B and N have been found to be *negative*. This assignment is consistent with the following theoretical consideration: All the possible perturbing levels must belong to the conduction states that are located *above* $\Gamma_{25'}$. If one postulates this, one must have a negative sign for each of the four different perturbation terms (F, G, H_1, and H_2 denoted in reference 1). Furthermore, only the combination of the experimental values A, B, and N all having negative signs is shown to fill the above requirement. In silicon, on the other hand, the assignment has not been unique: Both signs, negative and positive, have been equally possible for B, even if one assumes that the conduction states furnish the dominant perturbations. Under this assumption it only follows that both L and M should be negative, but the sign of B which depends on the difference, $L-M$, is not certain.

In view of the remaining ambiguity for the silicon valence band some efforts have been made to settle the question about the sign of B. Kane[7] has argued in an investigation of the structures of the valence bands in germanium and silicon far off the center, $\mathbf{k}=0$, that the combination of the experimental values A, $|B|$, $|N|$ with *positive* sign for B would cause the valence band edge of silicon to be located off $\mathbf{k}=0$, which is evidently unrealistic. His argument could not, however, be checked accurately because of the large uncertainty of the experimental values that existed in the earlier experiments.

Another approach to this problem has been to evaluate the parameters directly from first principles by solving the Schrödinger equation in crystals. Detailed theoretical calculations of the band structures of diamond-type crystals have been made by Herman, Woodruff, Kleinman-Phillips, and Bassani-Celli based on the orthogonalized plane wave method,[8] and by many authors based on the tight-binding approximation. All of these calculations have confirmed the assumption mentioned previously that the valence band top $\Gamma_{25'}$ lies *below* any of the four representations Γ_{15}, $\Gamma_{2'}$, and the other two.

Kleinman and Phillips,[8] who made a very elaborate calculation of the energy bands in silicon, have indicated the difference, $L-M$, to be *positive*.[9] Their calcu-

[6] A statement has been given by G. E. Pikus and G. L. Bir [Phys. Rev. Letters **6**, 103 (1961)] about the signs of the inverse mass parameters as well as the band-splitting deformation potentials for the silicon valence band. [Note that these authors have defined the deformation potentials with signs opposite to those of D_u and D_u': $b = -\frac{2}{3}D_u$ and $d = -(2/\sqrt{3})D_u'$.] They have expected that D_u and D_u' would have the same signs as those of the similar splitting parameters for acceptor ground states in silicon, so that the nature of the splitting of both the valence band top and the acceptor level would be the same. From the results of reference 4 it can now be seen that their expectation was indeed right. See also their related papers, of which references are given in Hensel and Feher's paper (reference 4).

[7] E. O. Kane, J. Phys. Chem. Solids **1**, 82 (1956).

[8] L. Kleinman and J. C. Phillips, Phys. Rev. **118**, 1158 (1960). Most of other references are given in this paper; another is F. Bassani and V. Celli, J. Phys. Chem. Solids **20**, 64 (1961). See also J. C. Phillips, Phys. Rev. **112**, 685 (1958).

[9] The order of the energy levels for the conduction states in silicon has now been re-examined by J. C. Phillips in connection with the present discussion, Phys. Rev. **125**, 1931 (1962). The present author wishes to thank Dr. J. C. Phillips for calling the author's attention to F. Herman's paper concerning "core shifts" in OPW calculations.

lation shows that the sign of $L-M$ is closely related to the relative position of the levels $\Gamma_{2'}$ and Γ_{15} in the conduction bands at $\mathbf{k}=0$, and their result indicating a positive sign for it is essentially a consequence of the fact that the calculated level $\Gamma_{2'}$ is much higher than that of the Γ_{15} (the energy difference between these two is estimated to be approximately 6 eV) in contrast with the case of germanium. They argue that the "effective" crystal potential that has primary importance in determining the relative order of energy levels for valence electrons is sensitive, in the course of self-consistent calculations, to the energy levels and the wave functions of the core states (through the core orthogonalization terms, or the repulsive potentials according to their terminology). The difference between the two terms, $E(\Gamma_{2'})-E(\Gamma_{15})$, largely depends upon one particular Fourier component of the potential, V_{220}, that has *positive* sign and is significantly large, because the orthogonalization term overcomes the true crystal-potential term. This leads to the quoted result: $E(\Gamma_{2'})-E(\Gamma_{15})=6$ eV. It is noted that a similar estimate is also given in Woodruff's work.[10]

Under these circumstances it is clear that the absolute assignment of B without recourse to any model for the ordering of the Γ levels is most desirable. We shall see that such a possibility can be found in a dependence of the cyclotron resonance frequency on the magnitude of the external stresses. The reasoning is discussed in detail in the next section.

3. SHIFTS DUE TO STRAIN-INDUCED ADMIXTURES

We begin by setting up Hamiltonians pertinent to cyclotron resonances of holes in the $\Gamma_{25'}$ band under the influence of spin-orbit interaction and external stress. We shall keep parallel to Hensel-Feher's paper.[4] Since $\Gamma_{25'}$ is a three-dimensional representation (without spin) of the space group $O_h{}^7$, the Hamiltonians can most generally be represented by 6×6 matrices. The spin-orbit interaction splits the sixfold degenerate $\Gamma_{25'}$ into fourfold degenerate states, denoted by $p_{3/2}$, which form the valence band edge, and twofold degenerate $p_{1/2}$ states. Under ordinary circumstances, therefore, the Hamiltonians can be written in 4×4 matrix forms with basis operators of the angular momentum $\mathbf{J}(J=\frac{3}{2})$ to represent the interactions *within* the $p_{3/2}$ multiplet. The resulting expressions for a strain Hamiltonian H_e and for an effective mass Hamiltonian H_k are presented in H-F[4] [Eqs. (6) and (7), respectively]. The 4×4 Hamiltonians, though convenient, do not suffice for the present purpose, since we need the off-diagonal part of H_e and H_k between the $p_{3/2}$ and $p_{1/2}$ multiplets.

Let us ignore for the moment the effect of the spin-orbit interaction that is responsible for the $p_{3/2}-p_{1/2}$ splitting. The Hamiltonians H_e and H_k can then be written conveniently in terms of another angular mo-

mentum operator, the orbital angular momentum $\mathbf{l}$ $(l=1)$, as

$$H_e = D_0(e_{xx}+e_{yy}+e_{zz})+D_1[(I_x{}^2-\tfrac{1}{3}I^2)e_{xx}+\text{c.p.}]$$
$$+D_2[2\{I_xI_y\}e_{xy}+\text{c.p.}], \quad (3.1)$$

$$H_k = A_0(k_x{}^2+k_y{}^2+k_z{}^2)+A_1[(I_x{}^2-\tfrac{1}{3}I^2)k_x{}^2+\text{c.p.}]$$
$$+A_2[2\{I_xI_y\}\{k_xk_y\}+\text{c.p.}], \quad (3.2)$$

respectively. Here, c.p. denotes cyclic permutations with respect to the indices x, y, z. Here, and in the rest of the paper, a product of two quantities in the curly bracket indicates the symmetrized product; thus

$$\{I_xI_y\}=\tfrac{1}{2}(I_xI_y+I_yI_x), \quad \{k_xk_y\}=\tfrac{1}{2}(k_xk_y+k_yk_x), \text{ etc.}$$
$$(3.3)$$

Another remark appropriate here will be the definition of the *conventional* strain components.[11] They are explicitly defined by

$$e_{\alpha\beta}=\frac{\partial u_\alpha}{\partial x_\beta}+\frac{\partial u_\beta}{\partial x_\alpha}, \quad (\alpha\neq\beta)$$

$$=\frac{\partial u_\alpha}{\partial x_\alpha}, \quad (\alpha=\beta)$$

where u and x are a displacement vector and a position vector in a unit cell of a lattice. If the usual strain-stress relations are inserted in (1), the expression for H_e becomes

$$H_e=\frac{D_0}{c_{11}+2c_{12}}(T_{xx}+T_{yy}+T_{zz})$$
$$+\frac{D_1}{c_{11}-c_{12}}\left[\left(I_x{}^2-\frac{I^2}{3}\right)T_{xx}+\text{c.p.}\right]$$
$$+\frac{D_2}{c_{44}}[2\{I_xI_y\}T_{xy}+\text{c.p.}], \quad (3.4)$$

where $T_{\alpha\beta}$ is a stress component, and c_{11}, c_{12}, c_{44} are the usual three elastic constants for a cubic crystal.

The form of the strain Hamiltonian in (3.1) or of the stress Hamiltonian in (3.4) is a consequence of cubic symmetry. The first term in (3.1) or (3.4), which represents a totally uniform shift of the energy of the six degenerate levels, $\Gamma_{25'}$, is expressed by the single irreducible representation of the strain or the stress. The second and the third terms generally give rise to splittings of the degenerate levels, where the two- and the three-dimensional irreducible representations of the strain or stress components that are involved transform like Γ_{12}, and $\Gamma_{25'}$, respectively. Thus, the strain or stress Hamiltonian set up here has only a phenomenological meaning: The three constants D_i $(i=0, 1, 2)$

---

[10] T. O. Woodruff, Phys. Rev. **103**, 1159 (1956), and in *Solid State Physics*, edited by F. Seitz and D. Turnbull (Academic Press Inc., New York, 1957), Vol. 4, p. 367.

[11] It is distinguished from a component of the strain tensor, $S_{\alpha\beta}=\frac{1}{2}(\partial u_\alpha/\partial x_\beta+\partial u_\beta/\partial x_\alpha)$.

there are empirical parameters to be fit. While the effective mass Hamiltonian of the form (3.2) has a well-established basis from band theory, the *strain* Hamiltonian does not. Recently, Whitfield has discussed such a basis within a one-particle framework.[12] From his theory the constants D_i may be obtained from the matrix elements of what is called deformation potential operators of the form: $\mathfrak{D}_{\alpha\beta} = -(1/m)p_\alpha p_\beta + U_{\alpha\beta}(r)$. In this formalism D_0, D_1, and D_2 can be written

$$D_0 = \tfrac{1}{3}\langle \Gamma_{25'}{}^x | \mathfrak{D}_{xx} + 2\mathfrak{D}_{yy} | \Gamma_{25'}{}^x \rangle,$$
$$D_1 = -\langle \Gamma_{25'}{}^x | \mathfrak{D}_{xx} - \mathfrak{D}_{yy} | \Gamma_{25'}{}^x \rangle, \qquad (3.5)$$
$$D_2 = -\langle \Gamma_{25'}{}^x | \mathfrak{D}_{xy} | \Gamma_{25'}{}^y \rangle,$$

respectively. The two deformation potential constants, D_1 and D_2, responsible for uniaxial distortions of the $\Gamma_{25'}$ states, may have an order of magnitude of 1 eV, and thus by a shear strain of order 10^{-3} they will yield a splitting energy $\sim 10^{-3}$ eV.

We now consider the effect of the spin-orbit interaction which yields the $p_{3/2}-p_{1/2}$ splitting, Λ. The value of Λ for silicon, $\Lambda = 0.044$ eV, is an order of magnitude larger than the stress-induced splitting discussed above. Thus, we usually deal with the projections of the Hamiltonians H_e and H_k, both expressed by the I operators, onto the $p_{3/2}$ space. It is quite straightforward to write down the projected portions of the Hamiltonians in terms of the J operators: One just makes the following substitutions[13]

$$(I_\alpha{}^2 - \tfrac{1}{3}I^2) \rightarrow \tfrac{1}{3}(J_\alpha{}^2 - \tfrac{1}{3}J^2), \quad \alpha = x, y, z$$
$$\{I_\alpha I_\beta\} \rightarrow \tfrac{1}{3}\{J_\alpha J_\beta\}, \qquad \alpha \neq \beta. \qquad (3.6)$$

Comparing the projected Hamiltonians so obtained with those in Eqs. (6) and (7) of H-F, we can establish the relationship between the parameters D_i, A_i and those defined in H-F:

$$D_0 = D_d{}^v, \quad D_1 = 2D_u, \quad D_2 = D_u', \qquad (3.7)$$
$$A_0 = A, \quad A_1 = -3B, \quad A_2 = -N. \qquad (3.8)$$

Hereafter, we shall use H-F's notation.

The projected part of the Hamiltonian, designated by H_{11}, is a 4×4 matrix contained in the form

$$\begin{bmatrix} H_{11} & H_{12} \\ H_{21} & H_{22} \end{bmatrix},$$

the latter being the (JM_J) representation of the 6×6 matrix Hamiltonian. It is not quite straightforward to treat the off-diagonal part, H_{12} or H_{21}. One needs the precise form of each element. In Table I the off-diagonal elements for some basis operators are tabulated. The correction of the energy for the $p_{3/2}$ multiplet to the second order in the off-diagonal part may be calculated

[12] G. D. Whitfield, Phys. Rev. **121**, 720 (1961).
[13] J. M. Luttinger, Phys. Rev. **102**, 1030 (1956).

by the formula

$$H^{(2)}(J = \tfrac{3}{2}) = (1/\Lambda)(H_{12}H_{21}), \qquad (3.9)$$

which is a 4×4 matrix. We will not pursue the perturbation approach in this general form, but will confine ourselves to cases of an external uniaxial stress along simple crystallographic directions.

To discuss cyclotron resonance of holes we first determine the levels split at $\mathbf{k} = 0$ by the combined effects of spin-orbit (s-o) interaction and the stress Hamiltonian. The effective mass Hamiltonian H_k will subsequently be included to give the energy bands in the vicinity of $\mathbf{k} = 0$ for each split level. When a static uniform magnetic field $\mathbf{H}$ is applied, the three components of the wave vector $\mathbf{k}$ must satisfy the commutation relations

$$[k_\alpha, k_\beta] = (e/i\hbar c)H_\gamma. \qquad (3.10)$$

This quantization rule leads to the formation of Landau levels whose energy spacing is of major interest in cyclotron resonance absorption.

For a uniaxial stress T applied in the [001] direction the Hamiltonian matrix, $H_0 = H_e + H_{s-o}$, to zeroth order in $\mathbf{k}$ is written in the (JM_J) representation

$$H_0 = \begin{bmatrix} \epsilon & 0 & 0 & 0 & 0 & 0 \\ 0 & -\epsilon & 0 & 0 & -\sqrt{2}\epsilon & 0 \\ 0 & 0 & -\epsilon & 0 & 0 & \sqrt{2}\epsilon \\ 0 & 0 & 0 & \epsilon & 0 & 0 \\ 0 & -\sqrt{2}\epsilon & 0 & 0 & -\Lambda & 0 \\ 0 & 0 & \sqrt{2}\epsilon & 0 & 0 & -\Lambda \end{bmatrix}, \qquad (3.11)$$

with $M_J = \tfrac{3}{2}, \tfrac{1}{2}, -\tfrac{1}{2}, -\tfrac{3}{2}, \tfrac{1}{2}, -\tfrac{1}{2}$

where

$$\epsilon = \tfrac{2}{3}D_u T/(c_{11} - c_{12}) = \tfrac{2}{3}D_u(s_{11} - s_{12})T. \qquad (3.12)$$

Here we have omitted the term representing uniform shifts of the energy due to the stress as well as to the spin-orbit interaction. In the matrix representation in (3.11) J is "quantized" along [001], i.e., along the stress axis. A similar expression can be obtained, when a uniaxial stress T is applied in the [111] direction. Here one chooses the quantization axis of J along [111] and simply replaces ϵ by ϵ' in (3.11) where

$$\epsilon' = \tfrac{2}{3}D_u'T/2c_{44} = \tfrac{1}{3}D_u's_{44}T. \qquad (3.13)$$

The secular equation satisfied for H_0 in (3.11) can be easily factored. Here the simple nature of the equation will be emphasized. The uniaxial stress T gives rise to a distortion of the cubic symmetry, $\Gamma_{25'}$. However, the axial symmetry is still retained in the interaction H_0, as can be seen from the operator forms

$$H_0 = \epsilon(3I_3{}^2 - 2) + \tfrac{1}{3}\Lambda \mathbf{I} \cdot \boldsymbol{\sigma} \quad \text{for} \quad T \| [001],$$
$$= \epsilon'(3I_{3'}{}^2 - 2) + \tfrac{1}{3}\Lambda \mathbf{I} \cdot \boldsymbol{\sigma} \quad \text{for} \quad T \| [111]. \qquad (3.14)$$

Here $\boldsymbol{\sigma}$ denotes the Pauli spin. The component of the total angular momentum, $\mathbf{J} = \mathbf{I} + \tfrac{1}{2}\boldsymbol{\sigma}$, along the stress direction, denoted by J_3 or $J_{3'}$ for $T \| [001]$ or $T \| [111]$, respectively, can be seen to commute with the Hamil-

TABLE I. Off-diagonal part H_{12} for some basis operators in the (JM_J) representation. Columns and rows are arranged as $J=\frac{3}{2}$, $M_J=\frac{3}{2}, \frac{1}{2}, -\frac{1}{2}, -\frac{3}{2}$, and $J=\frac{1}{2}$, $M_J=\frac{1}{2}, -\frac{1}{2}$, so that the angular momentum $\mathbf{J}$ is represented in the form

$$J_z = \begin{bmatrix} \frac{3}{2} & 0 & 0 & 0 \\ 0 & \frac{1}{2} & 0 & 0 \\ 0 & 0 & -\frac{1}{2} & 0 \\ 0 & 0 & 0 & -\frac{3}{2} \end{bmatrix}, \quad J_x+iJ_y = \begin{bmatrix} 0 & \sqrt{3} & 0 & 0 \\ 0 & 0 & 2 & 0 \\ 0 & 0 & 0 & \sqrt{3} \\ 0 & 0 & 0 & 0 \end{bmatrix} \quad \text{for} \quad J=\tfrac{3}{2};$$

$$J_z = \begin{bmatrix} \frac{1}{2} & 0 \\ 0 & -\frac{1}{2} \end{bmatrix}, \qquad J_x+iJ_y = \begin{bmatrix} 0 & 1 \\ 0 & 0 \end{bmatrix} \qquad \text{for} \quad J=\tfrac{1}{2}.$$

$2I_z{}^2-I_x{}^2-I_y{}^2$	$I_x{}^2-I_y{}^2$	$\{(I_x+iI_y)I_z\}$	$\{(I_x-iI_y)I_z\}$	$\{2I_xI_y\}$
$\begin{bmatrix} 0 & 0 \\ -\sqrt{2} & 0 \\ 0 & \sqrt{2} \\ 0 & 0 \end{bmatrix}$	$\begin{bmatrix} 0 & (\frac{2}{3})^{1/2} \\ 0 & 0 \\ 0 & 0 \\ -(\frac{2}{3})^{1/2} & 0 \end{bmatrix}$	$\begin{bmatrix} \dfrac{1}{\sqrt{6}} & 0 \\ 0 & -\dfrac{1}{\sqrt{2}} \\ 0 & 0 \\ 0 & 0 \end{bmatrix}$	$\begin{bmatrix} 0 & 0 \\ 0 & 0 \\ -\dfrac{1}{\sqrt{2}} & 0 \\ 0 & \dfrac{1}{\sqrt{6}} \end{bmatrix}$	$\begin{bmatrix} 0 & -i(\frac{2}{3})^{1/2} \\ 0 & 0 \\ 0 & 0 \\ -i(\frac{2}{3})^{1/2} & 0 \end{bmatrix}$

tonian H_0. Accordingly, every eigenstate can be specified first by the quantum number $M_J=J_3$ or $J_{3'}$. M_J will take the values $\pm\frac{3}{2}$ once and $\pm\frac{1}{2}$ twice. Hence, the states corresponding to $M_J=\pm\frac{1}{2}$ should be specified further by some means. Each energy is doubly degenerate (Kramers degeneracy) with M_J and $-M_J$. Thus, we can denote the eigenvalues for the three doublets by $E_{3/2}$, $E_{1/2+}$, and $E_{1/2-}$, respectively. $E_{1/2\pm}$ is chosen to satisfy $E_{1/2+}>E_{1/2-}$.

In Fig. 1 the three energy eigenvalues are shown against the external stress T. In the limit $T\to 0$ the two doublets with the terms $E_{3/2}$ and $E_{1/2+}$ will approach $\Lambda/3$, while the third one, $E_{1/2-}$, will approach $-2\Lambda/3$, thus yielding the spin-orbit separation Λ in the absence of the strain. In this limit the first two doublets collapse into four degenerate states, which can be specified by another quantum number $J=\frac{3}{2}$. These are the states that have been investigated by the previous cyclotron resonance experiments. The existence of the extra degeneracy with $J=\frac{3}{2}$ in the case of $T=0$ is, of course, a consequence of the spherical isotropy of the spin-orbit interaction. As a uniaxial stress is turned on, this isotropy is violated resulting in two things: (a) splitting of the terms $E_{3/2}$ and $E_{1/2+}$ with the separation 2ϵ or $2\epsilon'$, (b) mixing of the eigenstates $J=\frac{3}{2}$ with $J=\frac{1}{2}$.

It will be noted that the mixing of the states by the uniaxial distortion takes place only between the two doublets with $M_J=\frac{1}{2}\pm$, because M_J is still a "good" quantum number under the uniaxial distortion: there is no matrix element of the strain term in H_0 between two states with different values of M_J. [See the matrix in (3.11).] This is an important property that will enable one to distinguish the two eigenstates with the energies $E_{3/2}$ and $E_{1/2+}$. If the eigenvectors of the matrix H_0 corresponding to $E_{3/2}$ and $E_{1/2+}$ are denoted by $\varphi_{3/2}$ and $\varphi_{1/2+}$, respectively, they can be written in

the (JM_J) representation as

$$\varphi_{3/2} = \varphi_{J=3/2, M=3/2}, \tag{3.15}$$

$$\varphi_{1/2+} = u\varphi_{J=3/2, M=1/2} + v\varphi_{J=1/2, M=1/2}. \tag{3.16}$$

Here the amplitude (u,v) for $\varphi_{1/2+}$ will depend on the relative strength of the strain energy ϵ or ϵ' to the spin-orbit separation Λ, and will represent the degree of the mixing. For $\varphi_{3/2}$, on the other hand, there is no mixing by the uniaxial distortion.

The difference in the character of the mixing effect for $\varphi_{3/2}$ and $\varphi_{1/2+}$ is due entirely to the simple uniaxial nature of the Hamiltonians in (3.14), and hence is typical only for the particular crystallographic axes
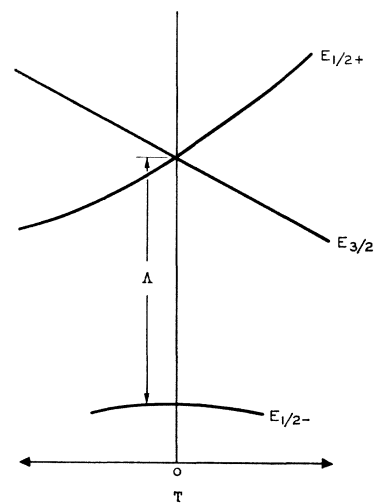

FIG. 1. Splitting of the valence states $\Gamma_{25'}$ by a spin-orbit interaction and by a uniaxial stress applied in the [001] or [111] direction. The energy term $E_{3/2}$ is represented by a straight line showing no mixing effect from the split-off state, while $E_{1/2+}$ is affected by the mixing.

[001] and [111] (or their equivalent axes). Except along these axes, the applied stress will cause, in general, a more complicated distortion. As an example, the case of a uniaxial stress T applied in the (001) plane will be examined. The strain Hamiltonian H_e is then written in terms of ϵ and ϵ' [defined in Eqs. (3.12), (3.13)] as

$$H_e = \text{const} + 3[\epsilon(I_x^2 \cos^2\varphi + I_y^2 \sin^2\varphi)$$
$$+ \epsilon'(I_x I_y + I_y I_x) \cos\varphi \sin\varphi]$$
$$= \text{const} + 3(\epsilon_1 I_1^2 + \epsilon_2 I_2^2),$$

where φ is the angle between the x direction and the stress direction. In the second equation ϵ_1 and ϵ_2 can be obtained from the secular equation

$$\begin{vmatrix} -\epsilon_i + \epsilon\cos^2\varphi & \epsilon'\cos\varphi\sin\varphi \\ \epsilon'\cos\varphi\sin\varphi & -\epsilon_i + \epsilon\sin^2\varphi \end{vmatrix} = 0. \qquad (3.17)$$

In this case the uniaxial nature is retained only when one of the roots of Eq. (3.17) vanishes. The condition is

$$(\epsilon^2 - \epsilon'^2)\sin^2 2\varphi = 0. \qquad (3.18)$$

We can see from the above equation that, if a simple uniaxial stress is applied along an arbitrary direction in the (001) plane, the resulting distortion is uniaxial only when the following relation is satisfied:

$$\epsilon = \pm\epsilon'. \qquad (3.19)$$

Making a similar analysis we can conclude that, if a simple uniaxial stress is applied along an arbitrary direction in the (110) plane, the resulting distortion is uniaxial only when

$$\epsilon'(\epsilon - \epsilon') = 0. \qquad (3.20)$$

In particular, if the relation $\epsilon = \epsilon'$ is satisfied, the resulting distortion is always uniaxial with respect to the applied stress axis. Except for these few special cases, every eigenvector of the Hamiltonian H_0 is more or less an admixture of all the (J,M_J) basis vectors.

The energy band that belongs to each level, $E_{3/2}$ and $E_{1/2\pm}$, can be calculated according to first-order perturbation theory by taking the expectation value of the Hamiltonian H_k over each of the eigenvectors $\varphi_{3/2}$ and $\varphi_{1/2\pm}$, respectively. Since every matrix element in H_k is quadratic in k_α, the resulting bands retain to this order a parabolic nature, whose effective masses and anisotropy may be determined experimentally by observing cyclotron resonance lines. For the case of a strong stress ($\epsilon,\epsilon' \gg$ thermal energy for a charge carrier) essentially one line will be observed, the one that is associated with the uppermost energy band, the holes in the other bands being, thereby, depopulated. In the vicinity near the point $\mathbf{k}=0$ the locations of the three bands will be determined solely by the locations of the three unperturbed energies. The question which energy is higher, $E_{3/2}$ or $E_{1/2+}$ ($E_{1/2-}$ is always the lowest by its definition), depends on the sign of the parameter ϵ or

ϵ', which, in turn, depends on the sign of the relevant deformation potential and the nature of the applied stress.

In Table II the character assignment of the uppermost eigenvector is indicated in connection with the signs of ϵ and D_u for the [001] stress. There the form of the energy band calculated is also given with and without the strain-induced shift. If one calculates the energy bands by omitting the off-diagonal element in the matrix of (3.11), one obtains

$$(\varphi_{3/2}, H_k \varphi_{3/2}) = (A + \tfrac{1}{2}B)k_\perp^2 + (A - B)k_{\shortparallel}^2, \quad (3.21)$$

and

$$(\varphi_{1/2+}, H_k \varphi_{1/2+}) = (A - \tfrac{1}{2}B)k_\perp^2 + (A + B)k_{\shortparallel}^2. \quad (3.22)$$

Inclusion of the off-diagonal element, i.e., the admixture of the spin-orbit split-off state ($J = \tfrac{1}{2}$), modifies Eq. (3.22) to

$$(\varphi_{1/2+}, H_k \varphi_{1/2+}) = (A - \tfrac{1}{2}BZ)k_\perp^2 + (A + BZ)k_{\shortparallel}^2 \quad (3.23)$$

while Eq. (3.21) remains unchanged. Here the quantity Z is a function of $x = \epsilon/\Lambda$, the degree of mixing, of the form

$$Z(x) = \frac{1}{2}\left(1 + \frac{1 - 9x}{(1 - 2x + 9x^2)^{1/2}}\right) \simeq 1 - 4x, \quad x \ll 1.$$

To first order of the stress, therefore, the inverse effective mass of the band $E_{1/2+}(\mathbf{k})$ varies linearly with the stress as

$$\hbar^2/2m_\perp = A - \tfrac{1}{2}B(1 - 4\epsilon/\Lambda),$$
$$\hbar^2/2m_{\shortparallel} = A + B(1 - 4\epsilon/\Lambda). \qquad (3.24)$$

Thus, the characteristic difference between the decoupled bands $E_{3/2}(\mathbf{k})$ and $E_{1/2+}(\mathbf{k})$ can be found in their stress dependence. An appreciable shift of the effective mass is expected with an increase of the applied stress in the resonance, if the line is associated with $M_J = \pm\tfrac{1}{2}$. On the other hand, no such shift can be expected, if the line is associated with $M_J = \pm\tfrac{3}{2}$. When analyzing experimental results, one first extrapolates the effective mass versus stress curve to the zero stress. This procedure will determine, without knowing the assignment of the band, only the absolute magnitude of B, since $E_{3/2}(\mathbf{k})$ and $E_{1/2+}(\mathbf{k})$ have a twin character in the limit $T \to 0$ regarding the sign of B. The unique determination of its sign is possible, therefore, only after recognizing the difference between the two bands, which is now available from the identification of the shift, i.e., the presence or absence of the strain-induced shift discussed above.

The analysis can be extended to other directions of the applied stress. Table II may also apply to the case $T\|[111]$, another possible direction that retains absolute uniaxial nature of distortion. Here one is concerned with another set of the parameters, ϵ', D_u', and N, for which the procedure is entirely similar to that for the case $T\|[001]$. For the [110] type stress the analysis is

TABLE II. The character assignment distinguishing the decoupled bands $E_{3/2}(\mathbf{k})$ and $E_{1/2+}(\mathbf{k})$ for the case of tetragonal distortions, $T\|[001]$. The case for $T\|[111]$ may also be obtained, if ϵ, D_u, and B are replaced by ϵ', D_u', and $\frac{1}{3}N$, respectively.

Uppermost eigenvector	$\varphi_{3/2}$	$\varphi_{1/2+}$
Sign of ϵ	$\epsilon>0$	$\epsilon<0$
Sign of D_u[a]	$D_u<0$	$D_u>0$
$E(\mathbf{k})$ (without shifts)	$(A+\frac{1}{2}B)k_\perp^2+(A-B)k_\|^2$	$(A-\frac{1}{2}B)k_\perp^2+(A+B)k_\|^2$
$E(\mathbf{k})$ (with shifts)	$(A+\frac{1}{2}B)k_\perp^2+(A-B)k_\|^2$	$(A-\frac{1}{2}BZ)k_\perp^2+(A+BZ)k_\|^2$
		$Z\approx1-4\epsilon/\Lambda$
Sign of B[b]	$B>0$	$B<0$

[a] The sign of D_u is opposite to that of ϵ, if the applied stress is compressive.
[b] The sign of B is opposite to that of D_u, if the uppermost decoupled band is oblate. See reference 5.

more complicated. The uniaxial nature generally no longer holds, so that the admixtures take place in all the eigenvectors. We give here the formulas for the first-order shifts of the three inverse masses for $T\|[110]$. The latter are given by H-F [see Eq. (25) of reference 4]. For the uppermost band

$$\Delta\left(\frac{\hbar^2}{2m_1}\right)=\frac{B}{2\Lambda}\left(\frac{3\epsilon'^2-\epsilon^2}{(\epsilon^2+3\epsilon'^2)^{1/2}}-\epsilon\right)-\frac{N}{2\Lambda}\left(\frac{2\epsilon\epsilon'}{(\epsilon^2+3\epsilon'^2)^{1/2}}-\epsilon'\right),$$

$$\Delta\left(\frac{\hbar^2}{2m_2}\right)=-\frac{B}{\Lambda}\left(\frac{3\epsilon'^2-\epsilon^2}{(\epsilon^2+3\epsilon'^2)^{1/2}}-\epsilon\right),\qquad(3.25)$$

$$\Delta\left(\frac{\hbar^2}{2m_3}\right)=\frac{B}{2\Lambda}\left(\frac{3\epsilon'^2-\epsilon^2}{(\epsilon^2+3\epsilon'^2)^{1/2}}-\epsilon\right)+\frac{N}{2\Lambda}\left(\frac{2\epsilon\epsilon'}{(\epsilon^2+3\epsilon'^2)^{1/2}}-\epsilon'\right),$$

where the signs of the roots are assumed to be positive. The axes 1, 2, and 3 are labeled as in H-F, i.e., $1\|[1\bar{1}0]$, $2\|[00\bar{1}]$, and $3\|[110]$.

Finally, some further details of the strain-induced mass shift are presented here to help its identification in experiments.

(a) We have tentatively estimated the magnitude of the deformation potentials to be 1 eV. This yields an estimate of the mixing parameter, $4|x|=4|\epsilon/\Lambda|=10^{-1}$, for a value of the strain $\frac{2}{3}T/(c_{11}-c_{12})=10^{-3}$.

(b) It will be important to note the anisotropic nature of the shifts. The sum of the three inverse effective masses is equal to $3A$. This "sum rule" can be seen to hold, even when the shifts are included. Thus,

$$\sum_{\alpha=1,2,3}\frac{\hbar^2}{2m_\alpha}=3A,\quad\text{or}\quad\sum_{\alpha=1,2,3}\Delta\left(\frac{\hbar^2}{2m_\alpha}\right)=0,\quad(3.26)$$

independent of the strength and the orientation of the stress. An inspection of Eqs. (3.24) and (3.25) proves this property. Thus, for the $T\|[001]$ and $T\|[111]$ cases the shift $\Delta(1/m_\|)$ is opposite to $\Delta(1/m_\perp)$, and twice as large. If experimentally established, such a characteristic will make the identification of the shift indisputable.

(c) For the [110] type stress the shifts are complex, as given by Eq. (3.25). However, it will help to con-

sider the following point: We have pointed out that, if one of the special relations $\epsilon=\pm\epsilon'$ or $\epsilon'=0$, shown in Eqs. (3.19) and (3.20), is fulfilled, the uniaxial nature of the distortion is then restored. In fact, if we set $\epsilon=\pm\epsilon'$ (with the $+$ sign corresponding to the case of isotropic distortion), Eq. (3.25) becomes

$$\Delta(\hbar^2/2m_1)=\Delta(\hbar^2/2m_2)=\Delta(\hbar^2/2m_3)=0\quad\text{when}\quad\epsilon>0,$$

and

$$\Delta(\hbar^2/2m_1)=-(\epsilon/\Lambda)(B\mp N),\quad\Delta(\hbar^2/2m_2)=(2\epsilon/\Lambda)B,$$
$$\Delta(\hbar^2/2m_3)=-(\epsilon/\Lambda)(B\pm N)\quad\text{when}\quad\epsilon<0.$$

(The upper and the lower signs are according to $\epsilon'<0$ and $\epsilon'>0$, respectively.) Thus, the two choices of the sign of ϵ are quite distinguishable in this case also.[14]

4. EFFECTS OF FOURTH-ORDER TERMS— A THEORY OF LINE SHAPE

In order to retain a high accuracy in analyzing experimental results to deduce the effective mass parameters one should consider all possible corrections to the lowest order frequency calculated in the preceding section. One of such corrections comes from the second-order perturbation of the kinetic energy term H_k (the effective mass Hamiltonian), and can be written as a sum of fourth-order terms in the three variables k_x, k_y, and k_z. Clearly, this effect is important when the applied stress is not strong so that the decoupling of the upper two bands is incomplete and their nonparabolic nature is significant. In the present section this correction will be estimated by taking the matrix elements of H_k in the 4×4 projected form

$$H_k=Ak^2-\begin{bmatrix}X & U^* & V^* & 0\\ U & -X & 0 & V^*\\ V & 0 & -X & -U^*\\ 0 & V & -U & X\end{bmatrix}.\qquad(4.1)$$

Here the representation is assumed to diagonalize the strain Hamiltonian H_e in the projected space $p_{3/2}$. The

[14] J. C. Hensel has informed the author that $|\epsilon|\approx|\epsilon'|$ is really the case in silicon (private communication and reference 4). It is then interesting to inquire about the presence or absence of the linear shifts; if $\epsilon>0$, the shifts are expected to be very small. This fact is demonstrated by a comparison between case i and case ii of reference 4, IV-C.

matrix elements X, U, and V are, in general, quadratic forms of the three wave vector operators k_α's.

For convenience two cases will be distinguished according to whether the highest Kramers doublet is $M_J = \pm\frac{3}{2}$, or $\pm\frac{1}{2}$. The second-order perturbation energy for it is then given by

Case I:

$$E_{3/2}^{(2)} = (1/\Delta E)(U^*U + V^*V),$$
$$E_{-3/2}^{(2)} = (1/\Delta E)(UU^* + VV^*),$$
(4.2)

Case II:

$$E_{1/2}^{(2)} = (1/\Delta E)(UU^* + V^*V),$$
$$E_{-1/2}^{(2)} = (1/\Delta E)(U^*U + VV^*),$$
(4.3)

respectively. ΔE in these equations represents the difference of the two unperturbed energies, and is assumed to be positive. In applying the above formulas the two quantities U^*U and UU^*, or V^*V and VV^*, are not equal to each other, because in the presence of the magnetic field the three variables k_x, k_y, and k_z are not commuting quantities but are subject to the relations given in Eq. (3.10). The difference between $E_{M_j}^{(2)}$ and $E_{-M_j}^{(2)}$, expressed by the commutators, $[U^*,U]$ and $[V^*,V]$, distinguishes the two states belonging to a Kramers doublet as a quantum effect in the magnetic field.

To proceed further one rewrites the first-order kinetic energy calculated in Sec. 3 in the form

$$E^{(1)} = E^{(1)}(n,k)$$
$$= \hbar\omega_0(n+\tfrac{1}{2}) + (\hbar^2/2m_l)k^2,$$
(4.4)

where n represents 0 or positive integers (Landau quantum number), and k represents the component of the wave vector along the $\mathbf{H}$ direction. The unperturbed frequency as well as the longitudinal effective mass m_l are assumed here to be positive quantities. Thus, for the present discussion, the scale in the energy diagram in Sec. 3 is now reversed, since all the energy bands discussed there are supposed to have negative curvatures at $\mathbf{k}=0$; and the second-order perturbation (4.2) or (4.3) must accordingly have the sign reversed.

The diagonal part of the kinetic energy up to second order can be written in a quadratic form of the two variables, n and k, and is denoted by $E(n,k)$. The frequency of the resonance induced by a dipole transition from nth Landau level to $(n+1)$th Landau level is then given by

$$\hbar\omega = E(n+1, k) - E(n,k).$$
(4.5)

The frequency ω generally depends on n and k^2 and can be written in the following form:

$$\omega_{n,k} = \omega_0 + \omega_1 + \omega_2 n + \omega_3 k^2.$$
(4.6)

The first term represents the unperturbed frequency, and the remaining three terms the corrections from the fourth-order parts.

By way of example the calculation will be shown in great detail in the simple case for the applied stress and magnetic field both parallel to the [001] direction. In this case, U and V are given by

$$U = \frac{1}{\sqrt{3}}Nk_z(k_x + ik_y), \quad V = \frac{\sqrt{3}}{2}B(k_x^2 - k_y^2) + \frac{i}{\sqrt{3}}N\{k_xk_y\}.$$
(4.7)

Using the commutation relations between k_x and k_y one can write

$$\tfrac{1}{2}[U^*,U] = \tfrac{1}{3}N^2k^2eH/\hbar c,$$
(4.8)

$$\tfrac{1}{2}[V^*,V] = BN(eH/\hbar c)^2(2n+1).$$
(4.9)

Also for the diagonal part of the product

$$\{U^*U\} + \{V^*V\} = \tfrac{3}{2}(B^2 + \tfrac{1}{9}N^2)(n^2 + n + 1)$$

$$\times \left(\frac{eH}{\hbar c}\right)^2 + \tfrac{1}{3}N^2(2n+1)k^2\frac{eH}{\hbar c}. \quad (4.10)$$

The contribution to the frequency from (4.10) is common to all the bands, while the contributions from (4.8) and (4.9) are different for each of the four M_J's. Dividing two cases, I and II, one can now explicitly write the four frequencies as follows:

Case I: (The $M_J = \pm\frac{3}{2}$ band is the highest, or $\epsilon > 0$.)

$$\hbar\omega_0 = 2(A + \tfrac{1}{2}B)eH/\hbar c,$$
$$\hbar\omega_1 = (3/-\Delta E)(B \pm \tfrac{1}{3}N)^2(eH/\hbar c)^2,$$
$$\text{according to } M_J = \pm\tfrac{3}{2}, \quad (4.11)$$
$$\hbar\omega_2 = (3/-\Delta E)(B^2 + \tfrac{1}{9}N^2)(eH/\hbar c)^2,$$
$$\hbar\omega_3 k^2 = (1/-\Delta E)\tfrac{1}{3}N^2k^2eH/\hbar c.$$

Case II: (The $M = \pm\frac{1}{2}$ band is the highest, or $\epsilon < 0$.)

$$\hbar\omega_0 = 2(A - \tfrac{1}{2}BZ)eH/\hbar c,$$
$$\hbar\omega_1 = (3/-\Delta E)(B \pm \tfrac{1}{3}N)^2(eH/\hbar c)^2,$$
$$\text{according to } M_J = \pm\tfrac{1}{2}, \quad (4.12)$$
$$\hbar\omega_2 = (3/-\Delta E)(B^2 + \tfrac{1}{9}N^2)(eH/\hbar c)^2,$$
$$\hbar\omega_3 k^2 = (1/-\Delta E)\tfrac{1}{3}N^2k^2eH/\hbar c.$$

The energy denominator ΔE is given by

$$\Delta E = 2|\epsilon|.$$
(4.13)

Therefore, all the correction terms ω_1, ω_2, and ω_3 are proportional to the inverse of the applied stress T.

At the absolute zero temperature the dipole transition is restricted to the one, $n=0$, $k=0 \rightarrow n=1$, $k=0$. The corresponding resonance frequency will then be given by

$$\omega = \omega_0 + \omega_1.$$
(4.14)

At a finite but still very low temperature the other terms ω_2 and ω_3 will also play roles in modifying the resonance line. The k-dependent term $\omega_3 k^2$ will give a continuous shift; thus effectively a broadening. This kind of broadening effect known as a k_z broadening is

important[15] in determining the correct frequency in the absence of stress (i.e., "quantum" spectra), where the magnitude of the term $\omega_3 k^2$ for thermal carriers is usually comparable with the unperturbed frequency. In the present case it turns out that the term $\omega_3 k^2$ does not yield a shift of the maximum of the intensity. This is confirmed by a direct integration of the intensity curves with respect to the continuous parameter, k.

The most significant modification that should be carefully examined arises from the first two terms ω_1 and ω_2. If the resolution of the microwave signal is high enough, many lines will be observed that correspond to different values of the initial Landau quantum number. Under ordinary circumstances an observed resonance will be a superposition of several lines, whose frequency shift will be determined by a certain statistical average of the individual terms with different n.

Both the corrections ω_1 and ω_2 are negative and diminish the unperturbed frequency ω_0. Therefore, the apparent resonance frequency for the superposed line must be lower than ω_0. To see their order of magnitude one rewrites ω_1 and ω_2, as

$$|\omega_1|/\omega_0 = \tfrac{3}{8}(m_\perp/m)^2(B \pm \tfrac{1}{3}N)^2 \hbar\omega_0/|\epsilon|, \qquad (4.15)$$

$$|\omega_2|/\omega_0 = \tfrac{3}{8}(m_\perp/m)^2(B^2 + \tfrac{1}{9}N^2)\hbar\omega_0/|\epsilon|, \qquad (4.16)$$

where the constants B and N are measured in units of $\hbar^2/2m$, and $\omega_0 = eH/m_\perp c$. The strain energy ϵ is estimated for $T = 2000$ kg cm^{-2} to be

$$|\epsilon| = \tfrac{2}{3}|D_u s T| = 2 \times 10^{-3} \text{ eV}. \qquad (4.17)$$

Here $s = 1/c_{11} - c_{12} = 1.0 \times 10^{-12}$ dyn cm^{-2}, and the deformation potential $|D_u|$ is assumed to be 1.5 eV. A more satisfactory estimate for D_u will be obtained in H-F. Also, their preliminary results indicate

$$|B| = 0.8, \quad |N| = 9.3, \quad m_\perp/m = 0.26.$$

Using these values, we can estimate the right-hand side of Eq. (4.15) to be

$$|\omega_1|/\omega_0 = 7.1 \times 10^{-3} \quad \text{when } B \text{ and } N \text{ are additive, and}$$
$$= 2.5 \times 10^{-3} \quad \text{when } B \text{ and } N \text{ are subtractive.}$$

Similarly, for the right-hand side of Eq. (4.16)

$$|\omega_2|/\omega_0 = 4.9 \times 10^{-3}.$$

In these estimates ω_0 is assumed to be equal to the microwave frequency: $\omega_0 = 2\pi \times 9000$ Mc/sec.

It is somewhat difficult to carry out the statistical average over the quantum number n for the ω_2 term in order to deduce its effective shift. One way of doing this is to plot numerically the individual lines and superpose them. This is done by assuming a Lorentzian shape for each line with a common width. The result is shown in Figs. 2 and 3. Here the intensity curve is understood to be as a function of the static magnetic

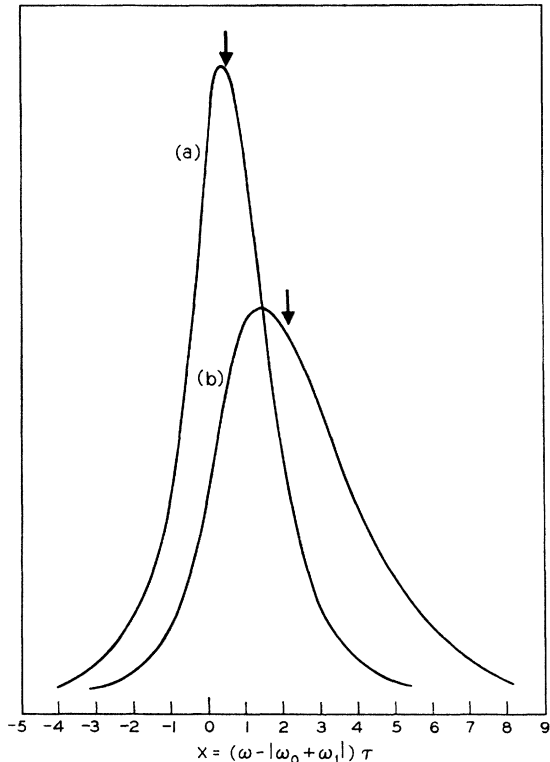[15] M. Okazaki (to be published).

FIG. 2. Theoretical curves of the hole resonance. Each curve is obtained as a superposition of the individual lines with different Landau quantum number. The individual line is assumed to be a Lorentzian. The weighting factor in the superposition is $(n+\tfrac{1}{2})e^{-\beta\hbar\omega_0(n+\tfrac{1}{2})}$ with $\beta\hbar\omega_0 = 0.34$ ($\omega_0 = 2\pi \times 9000$ Mc/sec, $\beta^{-1} = 1.3°$K): thus the expression for each curve is given by

$$y = \sum_{n=0} \frac{(2n+1)e^{-0.34(n+1/2)}}{1 + (x - |\omega_2|\tau n)^2}.$$

(a) $|\omega_2|\tau = 0.1$, (b) $|\omega_2|\tau = 0.4$. To secure convergence the summation is made up to $n = 20$ by a computer. The arrows indicate the estimated positions of the maximum points by Eq. (4.19).

field H to conform with usual experimental conditions. The intensity vs H dependence is regarded in the vicinity of the resonance as just the intensity vs ω dependence with the abscissa reversed at the point $\omega_0 + \omega_1$. This should not yield a significant error, since the individual shift, $\omega_2 n$, is quite small compared to ω_0. Besides a shift of the maximum for the superposed line we can see an asymmetry. Clearly, this asymmetry is a consequence of the accumulated intensity on the high mass side with many quantum numbers, thus forming a tail.

If the initial states can be assumed to have a Boltzmann distribution,[16] and if the width of the individual line is much greater than $\omega_2(\omega_2\tau \ll 1)$, the resulting shift

[16] The distribution depends upon the way of producing charge carriers, i.e., upon the wavelength of the light. It also changes by an increase of the microwave power. The present paper is not concerned with the problem of finding the best distribution. For analyzing experimental results it is desirable to eliminate heating processes as much as possible.
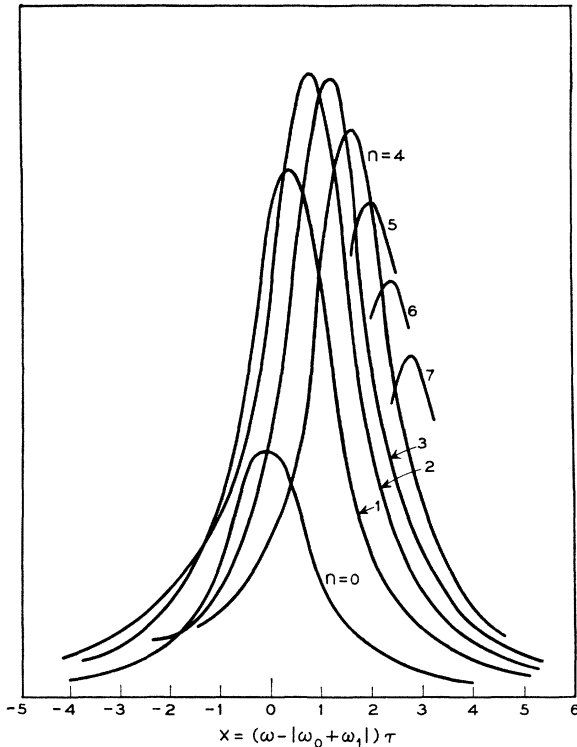
FIG. 3. Some individual lines in the series for curve (b) in Fig. 3.

for the superposed line can be approximately given by averaging $\omega_2 n$ over the Boltzmann distribution:

$$\Delta\omega = \omega_1 + \omega_2 \bar{n}, \quad \bar{n} = \sum_{n \geq 0} n w_n,$$

where

$$w_n = (n+\tfrac{1}{2})e^{-\beta\hbar\omega_0(n+1/2)} / \sum_{n \geq 0} (n+\tfrac{1}{2})e^{-\beta\hbar\omega_0(n+1/2)}. \quad (4.18)$$

This expression is derived by expanding a general form of the frequency-dependent conductivity tensor.[17] The factor $n+\tfrac{1}{2}$ in w_n is necessary because of the square of

---

[17] R. Kubo, J. Phys. Soc. Japan **12**, 570 (1957). The symmetric part of the conductivity was shown to be

$$\sigma_{xx}(\omega) = \frac{1}{2E_\beta(\omega)} \int_{-\infty}^{\infty} \langle \{j_x j_x(t)\} \rangle \cos\omega t \, dt.$$

Expanding the right-hand side into eigenmodes of the cyclotron motion, in which some damping factors are included, one reaches an expression essentially of the form

$$\sigma_{xx}(\omega) = \sum_{n=0} w_n g(\omega - \omega_n),$$

where $g(\omega)$ is the Lorentzian line-shape function. In deriving this, the factor $E_\beta(\omega) = \tfrac{1}{2}\hbar\omega \coth(\tfrac{1}{2}\beta\hbar\omega)$ is essential in giving the correct normalization for w_n. The maximum point of the composite line satisfies

$$\sum_n w_n \frac{d}{d\omega} g(\omega - \omega_n) = 0,$$

from which one can see that the shift coincides with the expression in (4.18) provided $\omega_2\tau \ll 1$.

the dipole matrix element. Using Eq. (4.18) one finds

$$\Delta\omega = \omega_1 + \omega_2 \left(\frac{1}{e^{\beta\hbar\omega_0}-1} + \frac{1}{\sinh\beta\hbar\omega_0} \right) \quad (4.19)$$

$$\approx \omega_1 + (2/\beta\hbar\omega_0)\omega_2 = \omega_1 + \omega_2 2k\Theta/\hbar\omega_0.$$

Thus, the contribution from ω_2 is now enhanced by the factor $2k\Theta/\hbar\omega$. One expects the total correction at the temperature $\Theta = 1.3 \, \mathrm{K}°$ to be

$$|\Delta\omega/\omega_0| \approx 3 \times 10^{-2}. \quad (4.20)$$

The shift of the second term is linear with temperature, and it can be checked in experiments. One can also calculate the second moment of the superposed line, which will provide a rough measure of the width due to the "inhomogeneous" broadening effect:

$$\langle \Delta\omega^2 \rangle_{av} = \omega_2^2 (\langle n^2 \rangle_{av} - \bar{n}^2) \approx 2\omega_2^2/\beta^2(\hbar\omega_0)^2. \quad (4.21)$$

Thus, the width of the observed line should also be linear with temperature, provided that the broadening is actually governed by the above mechanism. However, this is not certain, since another time constant τ, the relaxation time for individual lines, is not known at present. If the condition $\omega_2\tau \ll 1$ is really satisfied, the broadening should be determined by τ, and Eq. (4.21) may not apply.

To examine this point in more detail we quote in Table III the results of numerical computations for the line shape. Here the second and the fourth columns list, respectively, as a function of the parameter $|\omega_2|\tau$, the position of each superposed line maximum, x_{max}, and the half-width, Δx, on the reduced scale $x = (\omega - |\omega_0 + \omega_1|)\tau$. In Table III we compare these two quantities with the "approximate" first moment (4.19) and second moment (4.21). For the shift of the maximum it can be seen that the first moment value deviates significantly for all samples from the "true" shift x_{max} to higher values, the deviation being larger for larger value of $|\omega_2|\tau$. With the aid of Fig. 2 one can see that this overestimate of the shift by Eq. (4.19) is closely connected with the asymmetry effect, namely, a weighted contribution from the high-frequency side to the first moment. From this one expects that the first moment can indicate the correct shift of the maximum in the limit $|\omega_2|\tau \to 0$, as mentioned previously. For the width we employ a conventional assumption that the width is proportional to the square root of the second moment, $(\langle \Delta\omega^2 \rangle_{av})^{1/2}$, the proportionality constant being chosen for a Gaussian shape. Contrary to the case of the shift, the second moment value of the width deviates from the true width significantly for smaller $|\omega_2|\tau$, indicating the relative importance of the $1/\tau$ broadening in the total width. One can see that the computed half-width is close to the Gaussian half-width for samples $|\omega_2|\tau \gtrsim 0.4$; a fact which supports the analysis made in H-F (IV-E). It may not, however, entirely justify the linear dependence of the width upon temperature, since we

TABLE III. Comparison of first and second moments by Eqs. (4.19) and (4.21) with computed position of resonance maximum and half linewidth for $\Theta=1.3°K$ and $\omega_0=2\pi\times9000$ Mc/sec.

	Line maximum			Linewidth	
$\lvert\omega_2\rvert\tau$	x_{max}	$\lvert\omega_2\rvert\tau\times2k\Theta/\hbar\omega_0$	Δx	$2(\ln2)^{1/2}(2\langle\Delta\omega^2\rangle_{av})^{1/2}\tau$	
0.1	0.48	0.59	2.33	1.0	
0.2	0.86	1.18	2.92	2.0	
0.3	1.17	1.77	3.54	3.0	
0.4	1.46	2.36	4.18	4.0	
0.6	2.03	3.54	5.54	6.0	
0.8	2.51	4.72	6.79	8.0	

have not computed the line shapes at different temperatures. This point will be left to future investigations.

The calculation of ω_1 and ω_2 can be extended to other orientations of the applied stress and magnetic field. For another simple case, $T\|[111]$ and $H\|[111]$, U and V in the representation of (4.1) are given by

$$U=-\frac{1}{\sqrt{6}}\left(B-\frac{N}{3}\right)(k_1-ik_2)^2+\frac{1}{\sqrt{3}}\left(2B+\frac{N}{3}\right)$$
$$\times\{k_3(k_1+ik_2)\}, \quad (4.22)$$

$$V=\frac{1}{\sqrt{3}}\left(\frac{B}{2}+\frac{N}{3}\right)(k_1+ik_2)^2-\left(\frac{2}{3}\right)^{1/2}\left(B-\frac{N}{3}\right)$$
$$\times\{k_3(k_1-ik_2)\},$$

where the coordinates (1,2,3) are chosen so that 3 is parallel to the stress axis [111]. (The other two directions, 1 and 2, are along the [11$\bar{2}$] and [$\bar{1}$10] axes, respectively.) For this orientation

$$\lvert\omega_1\rvert/\omega_0=\tfrac{1}{6}(m_\perp'/m)^2(B+\tfrac{2}{3}N)^2\hbar\omega_0/\lvert\epsilon'\rvert,$$
$$\text{Case I}, \quad M_J=\tfrac{3}{2},$$
$$=\tfrac{1}{3}(m_\perp'/m)^2(B-\tfrac{1}{3}N)^2\hbar\omega_0/\lvert\epsilon'\rvert, \quad M_J=-\tfrac{3}{2},$$
$$=\tfrac{1}{2}(m_\perp'/m)^2(B^2+(2/9)N^2)\hbar\omega_0/\lvert\epsilon'\rvert,$$
$$\text{Case II}, \quad M_J=\tfrac{1}{2},$$
$$=0, \quad M_J=-\tfrac{1}{2},$$
$$(4.23)$$

$$\lvert\omega_2\rvert/\omega_0=\tfrac{1}{4}(m_\perp'/m)^2(B^2+(2/9)N^2)\hbar\omega_0/\lvert\epsilon'\rvert$$
$$\text{for all cases.} \quad (4.24)$$

The calculation of ω_2 is further extended to the case of H parallel to an arbitrary direction in the (1$\bar{1}$0) plane. Denoting the angle between T and H by θ, one obtains expressions for $\omega_2(\theta)/\omega_0$, which can be used for checking the anisotropies of the linewidths. For $T\|[001]$

$$\left(\frac{\omega_2}{\omega_0}\right)_\theta=\left(\frac{\omega_2}{\omega_0}\right)_{\theta=0}\left(\frac{m^*(\theta)}{m_\perp}\right)^2\frac{B^2f_1(\theta)+(N/3)^2f_2(\theta)}{B^2+(N/3)^2},$$

where

$$m^*(\theta)^2=\left(\frac{\cos^2\theta}{m_\perp^2}+\frac{\sin^2\theta}{m_\perp m_{\shortparallel}}\right)^{-1},$$

$$f_1(\theta)=\cos^2\theta, \quad (4.25)$$

$$f_2(\theta)=\frac{1}{4}\left[1+\left(1+\frac{m_\perp}{m_{\shortparallel}}\right)3\sin^2\theta+\frac{(1+3\sin^2\theta)3\cos^2\theta}{\cos^2\theta+(m_\perp/m_{\shortparallel})\sin^2\theta}\right];$$

and for $T\|[111]$

$$\left(\frac{\omega_2}{\omega_0}\right)_\theta=\left(\frac{\omega_2}{\omega_0}\right)_{\theta=0}\left(\frac{m^{*'}(\theta)}{m_\perp'}\right)^2\frac{B^2g_1(\theta)+2(N/3)^2g_2(\theta)}{B^2+2(N/3)^2},$$

where

$$m^{*'}(\theta)^2=\left(\frac{\cos^2\theta}{m_\perp'^2}+\frac{\sin^2\theta}{m_\perp'm_{\shortparallel}'}\right)^{-1},$$

$$g_1(\theta)=1+\frac{3}{8}\left(1+\frac{m_\perp'}{m}\right)\sin^2\theta+\frac{3\sqrt{2}}{4}\sin2\theta$$
$$+\frac{3}{8}\left(\frac{1-2\sqrt{2}\sin2\theta+7\sin^2\theta}{\cos^2\theta+(m_\perp'/m_{\shortparallel}')\sin^2\theta}\cos^2\theta-1\right), \quad (4.26)$$

$$g_2(\theta)=1+\frac{3}{8}\left(\frac{m_\perp'}{m_{\shortparallel}'}-1\right)\sin^2\theta-\frac{3\sqrt{2}}{8}\sin2\theta$$
$$+\frac{3}{8}\left(\frac{1+\sqrt{2}\sin2\theta+\sin^2\theta}{\cos^2\theta+(m_\perp'/m_{\shortparallel}')\sin^2\theta}\cos^2\theta-1\right).$$

For the case $T\|[111]$ the angle θ is to be taken positive for rotations of H toward the [001] axis. The anisotropy curves will be shown in H-F.

5. SUMMARY

From the calculations in the preceding two sections it is now clear that in the range of the external stress used in the experiment of H-F the stress-independent effective masses to be obtained from 4×4 matrix Hamiltonians to lowest order are subject to two major corrections, both in the order of magnitude 1~10%. An appropriate inclusion of these corrections in determining the effective mass can be made by assuming an empirical formula

$$1/m^*=1/m_0^*+\alpha T+\gamma/T,$$

for each principal effective mass. Here the first term on the right hand represents the zeroth-order inverse mass without stress dependence. The second and the third terms represent, respectively, the shift due to admixtures by the spin-orbit third band of Sec. 3, and the k^4 shift of Sec. 4. The nature of the constants α and γ has already been discussed. By way of summary we repeat some features here.

(1) α may have either a positive or negative sign depending upon the principal axis in question.

(2) γ must be always negative. It depends on temperature and on the external magnetic field.

(3) The first two terms are common to both components of a Kramers doublet (M_J and $-M_J$). The third term, on the other hand, generally differs for the two counterparts of the Kramers doublet by the field dependent correction to the frequency, i.e., the ω_1 term. Thus, a line may be resolved into two by the use of high-frequency cyclotron resonance techniques.

(4) α vanishes, if the resonance is associated with holes in the decoupled band $M_J = \pm\frac{3}{2}$.

(5) $\sum_{i=1,2,3}\alpha_i = 0$, where α_i are the components of α along the principal axes.

Actually, some reservation is required concerning the last two points, (4) and (5). It is related to some minor corrections to the zeroth-order inverse mass which have not been considered in the preceding sections. Here we consider briefly such minor effects.

(a) It is evident that the linear mass shift calculated in Sec. 3 comes from the cross terms between H_e and H_k in the perturbation formula. It can be seen, then, that the direct perturbation for H_k yields another k^4 term that is different from the one considered in Sec. 4 and smaller by the order of the magnitude of ϵ/Λ. For the simplest case, $T\|[001]$ and $H\|[001]$, the correction to the frequency is given by

$$\Delta(\omega_1/\omega_0) = -\tfrac{3}{4}(m_\perp/m)^2(B\pm\tfrac{1}{3}N)^2\hbar\omega_0/\Lambda,$$
$$\Delta(\omega_2/\omega_0) = -\tfrac{3}{4}(m_\perp/m)^2(B^2+\tfrac{1}{9}N^2)\hbar\omega_0/\Lambda, \qquad (5.1)$$

for $M_J = \pm\frac{3}{2}$, and by

$$\Delta(\omega_1/\omega_0) = \Delta(\omega_2/\omega_0) = -(m_\perp/m)^2 B^2\hbar\omega_0/\Lambda, \quad (5.2)$$

for $M_J = \pm\frac{1}{2}$. These expressions yield order-of-magnitude corrections less than 5×10^{-3} for microwave cyclotron resonances, and thus may be ignored. They cannot, however, be ignored for millimeter resonance.

(b) For the problem of the silicon valence band our starting Hamiltonians (3.1) and (3.2) are almost adequate, but not complete. First, from the symmetry point of view the expressions H_e and H_k are not completely general even to the lowest order in strain (or stress) and in $\mathbf{k\cdot p}$ perturbations. The ignored terms are spin dependent of the type, $e_{xx}I_x\sigma_x$, $e_{xy}(I_x\sigma_y+I_y\sigma_x)$; $k_x^2I_x\sigma_x$, $\{k_xk_y\}(I_x\sigma_y+I_y\sigma_x)$, etc. This type of coupling may result from the spin-orbit perturbation on the $\Gamma_{25'}$ and other Γ levels. In particular, the inverse effective mass parameters A, B, and N may be modified by this effect with corrections of the order Λ/E (band gap) $\sim2\%$.

(c) Another correction to the starting Hamiltonians can arise from the effect of a band gap change by the stress, and may be significant in the identification of the linear mass shift of Sec. 3, i.e., $4\epsilon/\Lambda$ or $4\epsilon'/\Lambda$. The effect can be described by the usual $\mathbf{k\cdot p}$ perturbation that is modified by the presence of the stress, thus, as one of the terms in a third-order perturbation form in which a $\mathbf{k\cdot p}$ element appears twice and a strain element appears once. The simplest and, probably, the largest contribution from such terms is the change of the inverse mass parameter by an isotropic volume dilation, where the deformation potential D_d of the order 10 eV may be involved. For example, from the conduction state $\Gamma_{2'}$ the effect yields a change of A that amounts to a maximum of $1\sim2\%$ with experimentally available stresses due to a linear shift of the form $\tfrac{1}{3}L(D_d^v-D_d^c)s_0T/E(\Gamma_{2'})-E(\Gamma_{25'})$. If such effects are taken into account, our conclusions (4) and (5) stated previously should not hold exactly: One expects the constant α not to vanish even for the $M_J = \pm\frac{3}{2}$ band and the "sum rule" not to hold. Such a deviation is expected, however, to be still a minor effect, and can be eliminated in the analysis of Sec. 3 since it is isotropic with respect to the $\mathbf{H}$ direction.